

Transitions between different superconducting states in mesoscopic disks.

V.A. Schweigert [[†]] and F.M. Peeters [[‡]]

*Departement Natuurkunde, Universiteit Antwerpen (UIA),
Universiteitsplein 1, B-2610 Antwerpen, Belgium*

Abstract

Using a linear analysis, we study the stability of giant-vortex states in very thin disks. The vortex expulsion and penetration fields are obtained for finite thickness disks from a numerical solution of the non-linear Ginzburg–Landau (GL) equations. Using an extension of the London approximation, in which the phase distribution of the order parameter is prescribed and the superconducting electron density is found numerically, we consider the free energy behavior for transitions between different superconducting states.

Key words: superconductivity, mesoscopics, vortex

Recently, much attention is devoted to investigations of superconducting phenomena in mesoscopic disks whose radius R and thickness d are comparable to the coherence ξ and penetration λ lengths. Precise measurements of the magnetization of single superconducting Al disks using Hall-magnetometry allowed to follow the evolution of few vortex states [1,2]. A number of remarkable observations (the influence of disk size on the *type* and *order* of the phase transition between the normal and the superconducting state, prominent hysteretic behavior in defect-free samples, the paramagnetic Meissner effect in the field-cooling regime, etc.) initiated several theoretical works, in which superconductivity of mesoscopic samples is considered within the full GL approach. The superconducting state may present either a giant vortex state with an axially symmetric distribution of the superconducting density or a multi-vortex Abrikosov-like state, which is usually realized in type-II superconductors. Since the effective penetration length $\lambda_\star = \lambda^2/d$ [3] may by far exceed that of a bulk superconductor, the multi-vortex states can also exist in thin disks made from type-I superconducting material.

The giant vortex states for finite thickness disks were considered in Refs.[4,5]. With increasing disk radius a second-order reversible phase transition from

the normal to the superconducting state observed for small disk radii is replaced by first-order transitions with jumps in the magnetization [4,5]. The simulated magnetizations are in good quantitative agreement with those from experiment [4,6,7]. The multi-vortex states have been investigated using the London approach [8], the GL approach [6,7,9], and the lowest Landau level approximation [10]. The free energy barriers separating the superconducting states with different vorticity were obtained using an expansion of the order parameter over the eigenfunctions of the GL kinetic energy operator [11]. The lowest Landau level approximation was used to study these barriers in Ref.[12]. An *equilibrium* phase diagram, showing which state is energetically preferable as function of the magnetic field and disk thickness, was found in Ref.[9]. In the present work, we study a *non-equilibrium* phase diagram showing the stability region of the giant vortex states as well as the *order* of the transition between different superconducting states.

We consider a superconducting disk surrounded by an insulator medium and placed in a uniform magnetic field H , which is perpendicular to the disk surface. Measuring the distance in units of the coherence length ξ , the vector potential \vec{A} in $\hbar c/2e\xi$, and the order parameter Ψ in $\sqrt{-\alpha/\beta}$ with α, β being the GL coefficients [3], we write the system of GL equations for a thin ($d \ll \xi, \lambda$) disk in the following form [9]:

$$\left(-i\vec{\nabla}_{2D} - \vec{A}\right)^2 \Psi = \Psi(1 - |\Psi|^2), \quad (1)$$

$$-\Delta_{3D}\vec{A} = \frac{d}{\kappa^2}\delta(z)\vec{j}_{2D}, \quad (2)$$

$$\vec{j}_{2D} = \frac{1}{2i} \left(\Psi^* \vec{\nabla}_{2D} \Psi - \Psi \vec{\nabla}_{2D} \Psi^* \right) - |\Psi|^2 \vec{A}, \quad (3)$$

where the indices $2D, 3D$ refer to two-dimensional (in the disk plane (x, y)) and three-dimensional operators; $\kappa = \lambda/\xi$ is the GL parameter; \vec{j}_{2D} is the density of superconducting current. The boundary conditions to Eqs. (1,2) correspond to zero superconducting current at the disk boundaries and an uniform external magnetic field far from the disk $\vec{A}_{|\vec{r}| \rightarrow \infty} = \frac{1}{2}[\vec{r} \times \vec{H}_0]$, respectively. Our numerical approach to solve Eqs.(1,2) is described in [9].

We restrict our considerations of the stability of the giant vortex states to the case of small disks $\lambda_* \gg R$, when the expulsion of the magnetic field can be neglected. Then the order parameter of the giant vortex state can be presented as $\Psi = \psi(\rho)e^{iL\phi}$, where L is the angular quantum momentum; ρ, ϕ are the cylindrical coordinates. The radial wavefunction ψ obeys the following equation

$$-\frac{1}{\rho} \frac{\partial}{\partial \rho} \rho \frac{\partial \psi}{\partial \rho} + \left(\frac{L}{\rho} + \frac{1}{2} H_0 \rho \right)^2 \psi = \psi - \psi^3, \quad (4)$$

with the boundary condition $(\partial\psi/\partial\rho)_{\rho=R} = 0$. In order to investigate whether the giant vortex state is stable with respect to small perturbations from other angular momentum states we use the time-dependent (TD) first GL equation [13]. Representing the order parameter as a mixture of three angular harmonics $\Psi = \psi(\rho)e^{iL\phi} + \delta_1(\rho)e^{iL_1\phi+\mu t} + \delta_2(\rho)e^{iL_2\phi+\mu t}$, we linearize the first TDGL equation with respect to small perturbations δ_1 , δ_2 and obtain the following set of equations

$$\begin{vmatrix} \hat{G}_{L_1} + 1 - 2\psi^2 & -\psi^2 \\ -\psi^2 & \hat{G}_{L_2} + 1 - 2\psi^2 \end{vmatrix} \cdot \begin{vmatrix} \delta_1 \\ \delta_2 \end{vmatrix} = \mu \begin{vmatrix} \delta_1 \\ \delta_2 \end{vmatrix}, \quad (5)$$

which describes our eigen-value problem. Here,

$$\hat{G}_L = -\frac{1}{\rho} \frac{\partial}{\partial \rho} \rho \frac{\partial}{\partial \rho} + \left(\frac{L}{\rho} + \frac{1}{2} H_0 \rho \right)^2$$

is the Schrödinger operator in an uniform magnetic field with the boundary condition $(\partial\delta_{1,2}/\partial\rho)_{\rho=R} = 0$. The sign of the eigenvalue μ determines whether the considered state is stable $\mu < 0$ or unstable $\mu > 0$. Note, that the use of three harmonics and the relation $L_1 + L_2 = 2L$ between them is dictated by the non-linear term in the RHS of Eq.(1), which corresponds to the third power of the order parameter. Generally, a linear analysis does not allow to predict which state will be realized from the evolution of instability. However, according to our previous results from solving the non-linear GL equations [9] we expect that the perturbation with $L_1 = 0$, $L_2 = 2L$ leaves the vorticity unchanged and leads to the appearance of a state corresponding to L vortices arranged in a ring. When the angular momentum of the perturbation is not a multiple of that of the initial state, we expect the appearance of a superconducting state with a different vorticity. To find the perturbation spectrum we use a finite-difference representation of the Schrödinger operator \hat{G} [5] and reduce Eq.(5) to a matrix, which is numerically diagonalized with the Householder technique. The state becomes unstable if the maximum value of μ found for different pairs $L_1, L_2 = 2L - L_1$ changes its sign and becomes positive.

The results from our linear analysis are shown in Fig. 1 for $L = 0, \dots, 9$. The Meissner state becomes unstable relative to the entrance of extra vortices with increasing magnetic field above the penetration field H_p . For small disk radii, it is the perturbation with $L_1 = L - 1$, $L_2 = L + 1$ which makes the L state unstable. With further increasing the disk radius, our linear analysis shows that a couple of vortices will enter the system at once. The points, at which the number of penetrating vortex changes, are denoted by solid squares in Fig. 1. A similar behavior of vortex penetration is also observed for the single vortex state. It should be noted, that the eigenvalues of the perturbations

with different angular momenta are very close to each other at large disk radii. Therefore, a non-linear consideration is required to answer how many vortices can simultaneously enter into the disk. Unfortunately, such an analysis is a very difficult task since the results turn out to be very sensitive to the shape of the perturbation. Our numerical solution of the non-linear GL equations shows that occasionally several vortices enter indeed into the system. Although we are able to predict the entrance field with high accuracy, the number of penetrating vortices is rather uncertain. This indicates that at the entrance field the barriers separating the different L -states become very small.

The Meissner state and the single vortex state can exist in arbitrary large disks. The expulsion field H_e , below which the vortex state becomes unstable relative to the transition to the Meissner state, decreases with disk radius, in such a way that the external magnetic flux piercing the disk tends to the flux quantum $\Phi_0 = hc/2e$. The other giant vortex states remain stable only inside some region of the phase diagram. Their stability is restricted by either the transition to the multi-vortex state with the same vorticity, which occurs as a rule with decreasing magnetic field, or the transition to another giant vortex state. The left (right) boundary of the stability region corresponds to expulsion (penetration) of a single vortex with decreasing (increasing) disk radius. Note, that the state with $L = 2$ in principle allows for a reentrant behavior - the transition to the multi-vortex state with both decreasing and increasing magnetic field. Unfortunately, this prediction is not confirmed by our non-linear analysis. The boundary of transition between the giant and multi-vortex state increases with angular momentum and, as expected, tends to saturate at the second critical field H_{c2} for large disk radii. The stability regions of different states overlap strongly and many different superconducting states can exist with the same external conditions.

To study the influence of the disk thickness on the penetration and expulsion field we solve numerically Eqs. (1,2). Starting from the Meissner (vortex) state we increase (decrease) slowly the applied magnetic field. Using the superconducting state obtained at the previous step as initial condition, we find a new steady-state solution of Eqs. (1,2) and check whether the vorticity changes. The penetration and expulsion fields found for zero disk thickness coincide with those from the linear analysis above. It turns out that the vortex state exhibits a weak paramagnetic Meissner effect just before vortex expulsion. This is the main reason why the expulsion field (thin dotted curves in Fig. 2) decreases with disk thickness. The Meissner state shows, as expected, a strong diamagnetic response. The decrease of the total magnetic flux piercing through the disk results in an expansion of the stability region of the Meissner state with increasing d/λ^2 . Recall, that the field expulsion from thin disks is only determined by the ratio d/λ^2 , which accounts for both the disk thickness and the penetration length of bulk material. The first critical field H_{c1} , above which the vortex state becomes energetically more favorable, also increases with the

disk thickness. All the critical fields $H_{c1} = 2H_{c2}\xi/R$, $H_e = 2H_{c2}\xi^2/R^2$, and $H_p = 2H_{c2}\xi\ln(R/\xi)/R$ can be found within the London approximation in the limit of zero disk thickness [8,11]. Note, that the penetration field from the London approximation does not agree with that from the GL theory because the saddle point state for vortex entrance does not correspond to any vortex state nearby H_p [11]. However, the London approach predicts rather accurately the expulsion and the first critical field for $R \gg \xi$ disk radii.

The superconducting density is assumed to be a constant in the conventional London approximation. This assumption breaks down at small disk radii or small inter-vortex distances which is the case of mesoscopic samples. An extension of the London approach accounting for variation of the amplitude ψ of the order parameter $\Psi(\vec{\rho}) = \psi(\vec{\rho})e^{iS(\vec{\rho})}$ has been proposed in [11]. The phase distribution S , which depends on the vortex positions $\vec{\rho}_i$, is assumed to be created by the vortices and their mirror images with coordinates $\vec{\rho}_i$ and $\vec{\rho}_i R^2/\rho_i^2$, respectively [8,11]. Then the amplitude of the order parameter obeys the first GL equation

$$-\Delta\psi + (\vec{\nabla}S - \vec{A})^2\psi = \psi - \psi^3, \quad (6)$$

with the boundary condition $(\partial\psi/\partial\rho)_{\rho=R} = 0$. Solving numerically the last equation we find the free energy $F(\vec{\rho}_i) = -\int \psi^4 d\vec{r}/\pi dR^2$, where integration is performed over the disk volume. Doing so we reduce the GL free energy functional defined in the functional space to the functional of the vortex coordinates. Then the vortices can be considered as classical particles, whose motion is governed by this free energy. Such an approach, which we call the modified London approach below, is shown to lead to accurate results in the case when vortices do not cross the sample boundary [11].

According to numerical simulations [9], the transition from the giant vortex state to the multi-vortex state with the same vorticity is followed by a weak jump in the slope of the magnetization indicating a second-order transition. The modified London approach allows to study the free energy as function of the vortex coordinates, which is shown in Fig. 3 for the two-vortex state. At large magnetic fields, the minimum of the free energy is achieved when both vortices are located in the disk center. With decreasing magnetic field, the curvature of the potential curve decreases and tends to zero at some critical point $H/H_{c2} \approx 0.58$. Thereafter, the multi-vortex state with separated vortices becomes more energetically favorable. No two minima of the free energy exist simultaneously. This agrees with results from our numerical solution of the GL equations [9] and proves that the transition is of second-order.

At small disk radii, all the multi-vortex state correspond to vortices arranged in a ring. With increasing disk radius, the configuration $(1 : L-1)$ with a single vortex inside the ring also becomes stable at large vorticity and coexists with

the ring structure $(0 : L)$ [14]. There is experimental evidence of such a coexistence [16]. Solving numerically Eqs. (1,2) we find the magnetization of both state $(0 : 7)$, $(1 : 6)$ (see Fig. 4). For $R = 5\xi$, the state with $(0 : 7)$ turns out to be energetically preferable. Note, that the magnetization curves do not merge with each other suggesting a first-order transition between these multi-vortex states. To find the free energy barrier separating the states $(1 : 6)$, $(0 : 7)$ we apply the modified London approach. Starting from the configuration $(1 : 6)$ we move slowly the central vortex to the disk boundary. The coordinates of the other vortices are found by minimizing the free energy. At small magnetic fields, there exists two minima of the free energy separated by a barrier (see Fig. 5). At some critical field $H/H_{c2} \approx 0.82$ this barrier disappears and the state $(1 : 6)$ becomes unstable. The transition between states $(1 : 6)$ and $(0 : 7)$ is followed by a jump in both the magnetization and the free energy which also proves the first-order of the transition between the multi-vortex states. Note, that the barrier separating two multi-vortex states is much smaller than that for vortex expulsion and penetration.

We thank A.K. Geim for useful discussions. This work is supported by the Flemish Science Foundation (FWO-VI) and the “Interuniversity Poles of Attraction Program - Belgian State, Prime Minister’s Office - Federal Office for Scientific, Technical and Cultural Affairs”. One of us (FMP) is a research director with the FWO-VI.

References

- [†] Permanent address: Institute of Theoretical and Applied Mechanics, Russian Academy of Sciences, Novosibirsk 630090, Russia.
- [‡] Electronic mail: peeters@uia.ua.ac.be
- [1] A.K. Geim, I.V. Grigorieva, S.V. Dubonos, J.G.S. Lok, J.C. Maan, A.E. Filippov, and F.M. Peeters, *Nature* **390**, 259 (1997).
- [2] A.K. Geim, S.V. Dubonos, J.G.S. Lok, M. Henini, and J.C. Maan, *Nature* **396**, 144 (1998).
- [3] P.G. de Gennes, *Superconductivity of metals and alloys*, (Addison-Wesley, N.Y., 1989).
- [4] P.S. Deo, V.A. Schweigert, F.M. Peeters, and A.K. Geim, *Phys. Rev. Lett.* **79**, 4653 (1997).
- [5] V.A. Schweigert and F.M. Peeters, *Phys. Rev. B* **57**, 13817 (1998).
- [6] P.S. Deo, V.A. Schweigert, and F.M. Peeters, *Phys. Rev. B* **59**, 6039 (1999).
- [7] P.S. Deo, F.M. Peeters, and V.A. Schweigert, *Superlatt. and Microstruct.* **25**, 1195 (1999).

- [8] A.I. Buzdin and J.P. Brison, Phys. Lett. A **196**, 267 (1994).
- [9] V.A. Schweigert, F.M. Peeters, and P.S. Deo, Phys. Rev. Lett. **81**, 2783 (1998).
- [10] J.J. Palacios, Phys. Rev. B. **58**, 1 (1998); *ibid*, Physica B **256-258**, 610 (1998).
- [11] V.A. Schweigert, F.M. Peeters, and P.S. Deo, Phys. Rev. Lett. **83** (1999).
- [12] J.J. Palacios, cond-mat/9908341 (1999).
- [13] C.R. Hu and R.S. Thompson, Phys. Rev. B **6**, 110 (1972).
- [14] Our studies of large disks $R/\xi = 8$ show the existence of a number of different stable configurations of the multi-vortex state with large vorticity. Similar to clusters of classical particles [15], these configurations have a shell structure with different shell occupation numbers.
- [15] V.M. Bedanov and F.M. Peeters, Phys. Rev. B **49**, 2667 (1994).
- [16] A.K. Geim, private communication

Fig. 1. The stability region of the different giant vortex states for zero disk thickness. The upper and lower solid thick curves correspond to the nucleation (H_{c3}) and expulsion (H_e) field, respectively. The thick-dashed curves denote the penetration fields (H_p) for the Meissner state and the single vortex state. The thin solid and dotted curves correspond to the transitions between the giant vortex states with different angular momenta and the transition from the giant vortex state to the multi-vortex state with the same vorticity (see inset) , respectively.

Fig. 2. The first critical (H_{c1}), penetration (H_p), and expulsion (H_p) field as function of the disk radius for different disk thicknesses. Thick curves denote results found with a conventional London approach.

Fig. 3. The free energy of the two-vortex state as a function of the inter-vortex distance (a) for different magnetic fields.

Fig. 4. The unitless magnetization $M = \int (H - H_0) d\vec{\rho} / 4\pi^2 H_{c2} R^2$ of the multivortex state $L = 7$ for two different vortex configurations and two thicknesses of the disk. The calculated magnetization includes the detector size effect [7] (square detector with width $\approx 3.1\mu m$).

Fig. 5. The free energy as a function of the position of one of the vortices, which is shifted from the disk center to the disk boundary. The inset shows the vortex configurations in the two stable states.

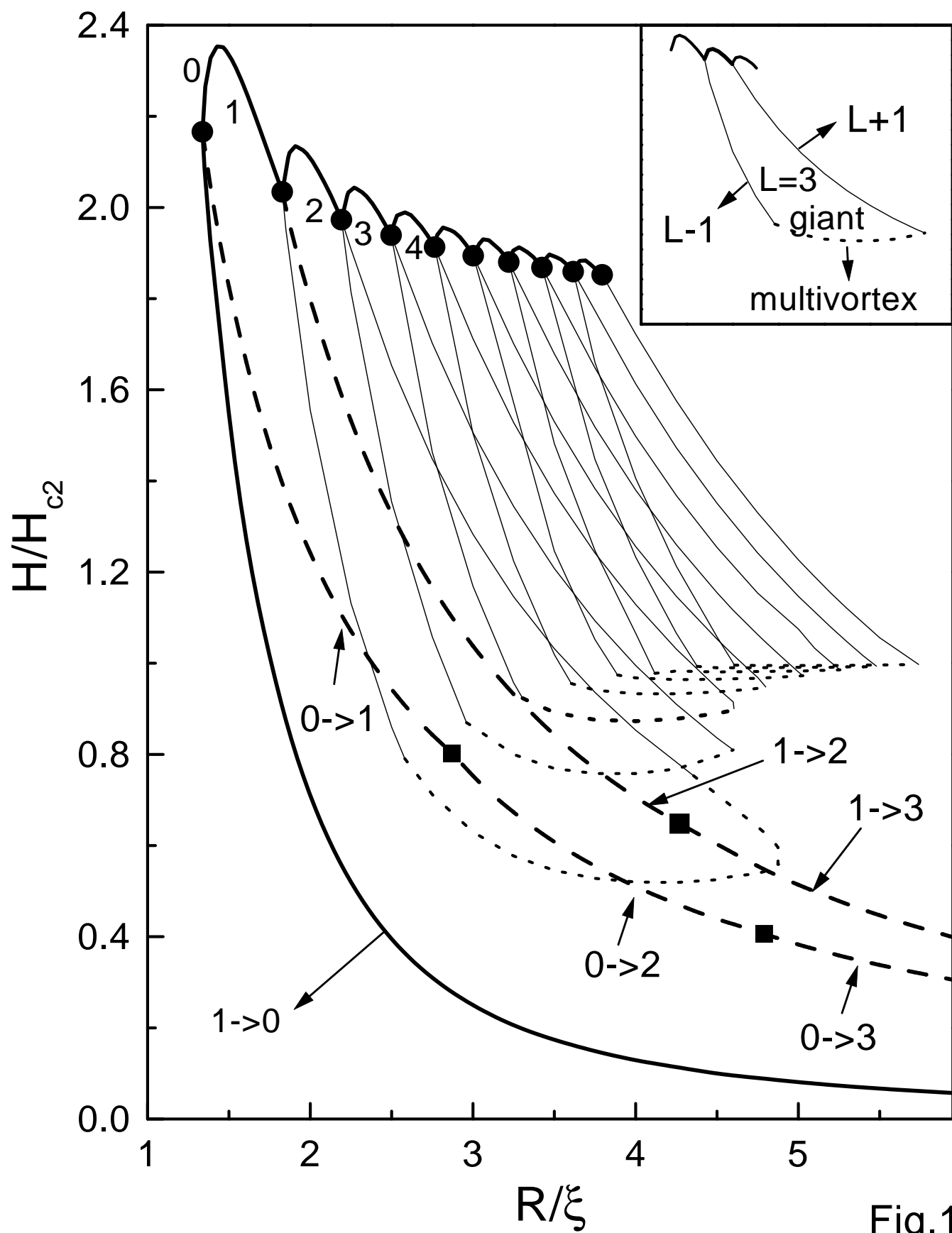


Fig.1

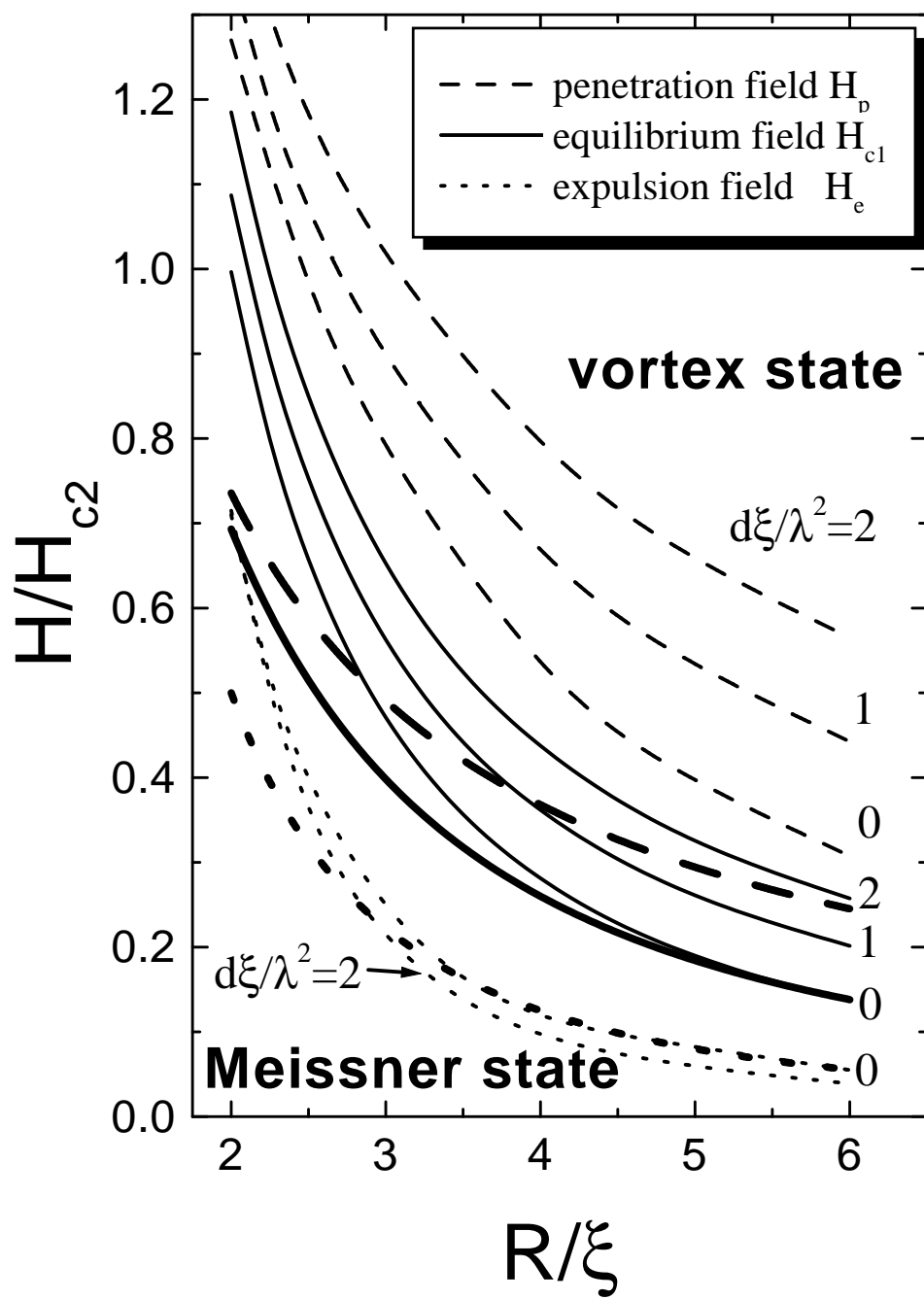


Fig.2

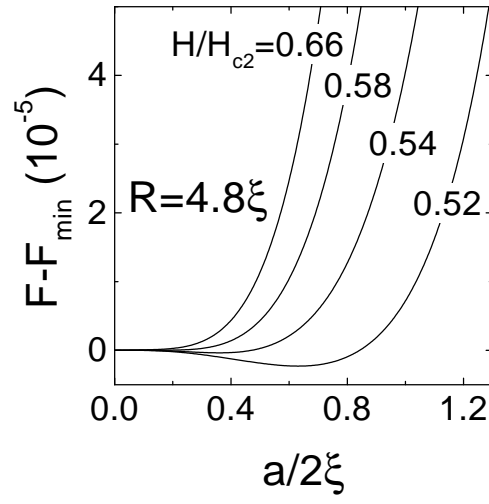


Fig.3

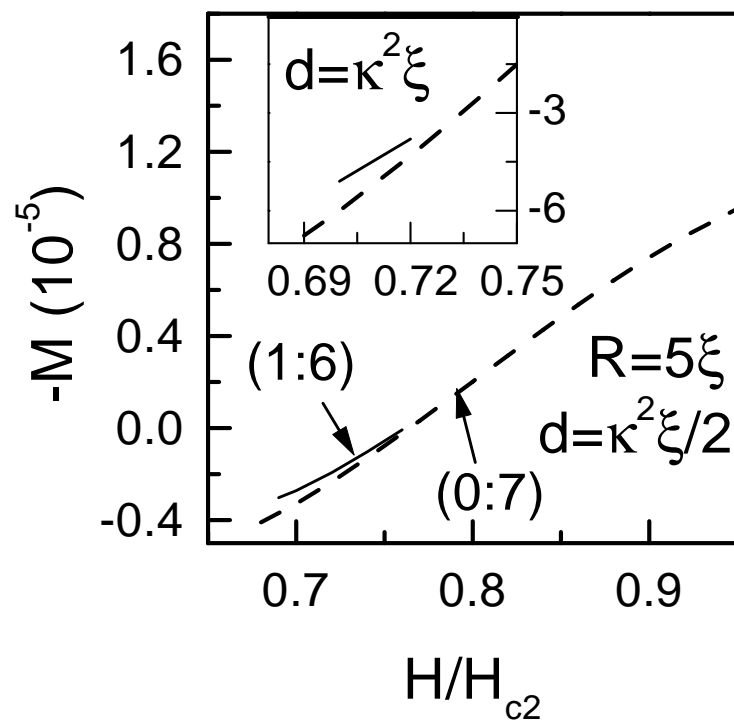


Fig.4

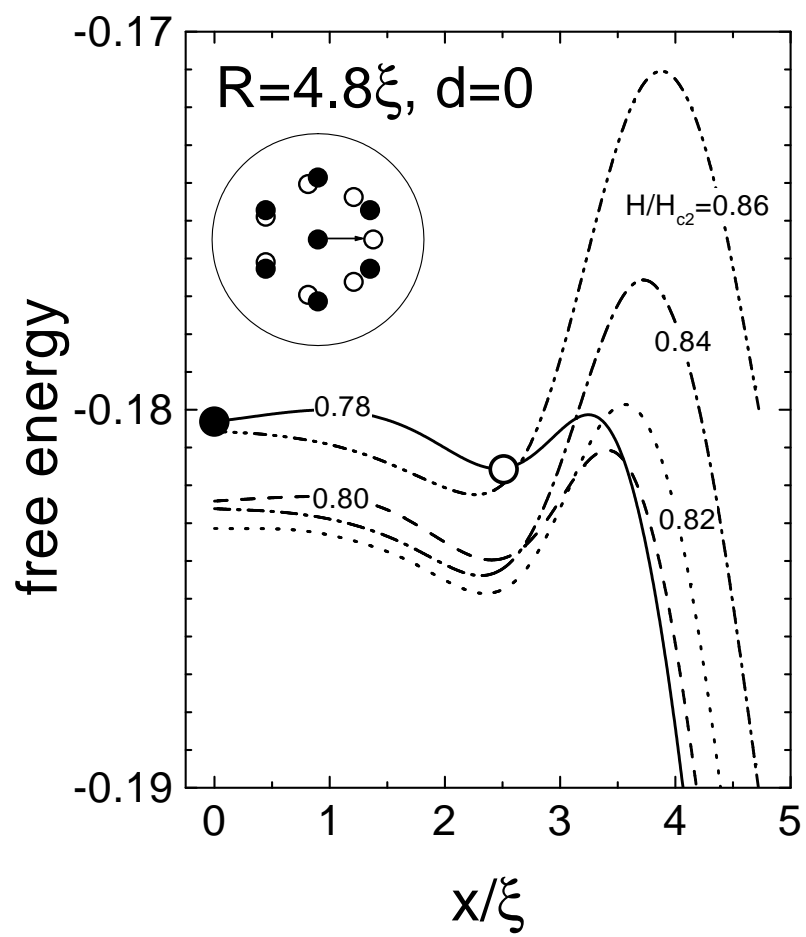


Fig.5